

Developing Simulation Models for Soft Robotic Grippers in Webots

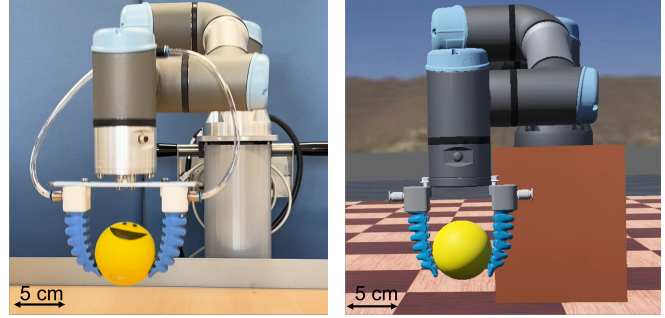
Yulyan Wahyu Hadi*^{1,2}, Lars Hof*¹, Bayu Jayawardhana¹, and Bahar Haghghat¹

Abstract—Robotic simulators provide cost-effective and risk-free virtual environments for studying robotic designs, control algorithms, and sensor integrations. They typically host extensive libraries of sensors and actuators that facilitate rapid prototyping and design evaluations in simulation. The use of the most prominent existing robotic simulators is however limited to simulation of rigid-link robots. On the other hand, there exist dedicated specialized environments for simulating soft robots. This separation limits the study of soft robotic systems, particularly in hybrid scenarios where soft and rigid subsystems co-exist. In this work, we develop a lightweight open-source digital twin of a commercially available soft gripper, directly integrated within the robotic simulator Webots. We use a Rigid-Link-Discretization (RLD) model to simulate the soft gripper. Using a Particle Swarm Optimization (PSO) approach, we identify the parameters of the RLD model based on the kinematics and dynamics of the physical system and show the efficacy of our modeling approach in validation experiments. All software and experimental details are available on github: <https://github.com/anonymousgiter1/Robosoft2025>.

I. INTRODUCTION

Soft robots are primarily constructed from highly flexible materials and often draw inspiration from the mechanical behavior of living organisms [1]. Researchers attempt to fabricate soft robots by mimicking the compliance and morphology of living creatures, with elastic bodies [2] and compliant actuation [3], such as soft grippers [4] [5] [6], soft manipulator [7], and soft robotic fish [8]. The inherent softness and low mechanical resistance of soft robots allow them to interact safely with delicate objects and adapt passively to complex surfaces. Multiple physics-based robotic simulators exist for traditional rigid-link robots, such as Gazebo [9] and Webots [10], which provide powerful tools for designing both the hardware and control of these robots, including integration with various kinds of virtual sensors, actuators, and other simulated robots. However, these do not support the simulation of soft robots, limiting the potential for systematic design and development in this field. This also limits the study of hybrid systems of soft and rigid robots within the same simulation environment.

Previous studies have explored standard solid mechanics discretization methods like Finite Element Analysis (FEA) [12] and voxel-based discretization [13] to simulate soft robots. Other approaches, including the Cosserat rod theory



(a) A pair of the real soft grippers mounted on a UR3e robotic arm. (b) A pair of the simulated soft grippers mounted on a simulated UR3e robotic arm in Webots. Pressurized air pipes are visible.

Fig. 1: Soft gripper attached to the UR3e robotic arm shown in the real setup and in the Webots simulation environment. The soft gripper is commercially available [11].

[14] and the piece-wise constant curvature (PCC) approach [15], have also been studied to simulate soft robots' behavior. Data-driven approached also has been employed to model the kinematics of the soft gripper [16]. However, these methods mainly serve as Computer-Aided Design (CAD) tools rather than comprehensive simulation environments for robots. Several dedicated simulation environments have been developed to simulate soft robots' behavior, such as SOFA [17], primarily targeted at real-time physical simulation, and SoMo [18], a framework based on pyBullet. Mujoco [19], a general-purpose efficient physics engine designed to advance research and development in robotics, offers fluid dynamic simulation capabilities that are also usable for soft robot simulations. Other example of simulation environment include toolboxes within MATLAB that have been developed particularly for soft robotics simulation such as Sorotoki [20], which facilitate the development of soft robots by providing a comprehensive set of tools for design, modeling, and control, and also SoRoSim [21], that uses the Geometric Variable Strain (GVS) approach to provide a unified framework for the modeling, analysis, and control of soft robots. All of these simulation environments lack the comprehensiveness of full-fledged robotic simulators with integrated sensors, actuators, and environment modeling.

In this study, we focus on pneumatically actuated beam-like soft grippers, a well-established category of soft robots [4] [6]. We present a computationally lightweight physics-based simulation model for beam-like soft grippers, directly integrated within the Webots robotic simulator. This integration provides access to Webots's extensive sensor and actua-

*Authors with equal contribution.

¹Y. Hadi, L. Hof, B. Jayawardhana, and B. Haghghat are all with the Faculty of Science and Engineering, University of Groningen, 9747 AG Groningen, The Netherlands y.w.hadi@rug.nl, l.hof@student.rug.nl, b.jayawardhana@rug.nl, bahar.haghghat@rug.nl

²Y. Hadi is also with the School of Electrical Engineering and Informatics, Bandung Institute of Technology, Indonesia

tor libraries. Furthermore, it offers capabilities of integrating soft and rigid robots, such as UR3e arm manipulator, within the same simulation environment, as shown in Figure 1b.

Firstly, we show how we model the structure of the soft body of a beam-like soft gripper via a Rigid-Link-Discretization (RLD) approach. The soft grippers are modeled as a series of rigid links, where each link is described by a mass-spring-damper system and is connected via joints to its neighboring links. Such a discretization method can readily be implemented in all open-source robotic simulation platforms. Secondly, we present an automated systems identification process based on dynamical data of the physical systems to create a digital twin instance of the physical soft grippers reducing the disparity between the simulation and reality. We use a heuristic search method, the Particles Swarm Optimization (PSO) algorithm to obtain a set of optimized parameters. Finally, we validate the accuracy of our simulation model using experimental data that are not used for systems identification.

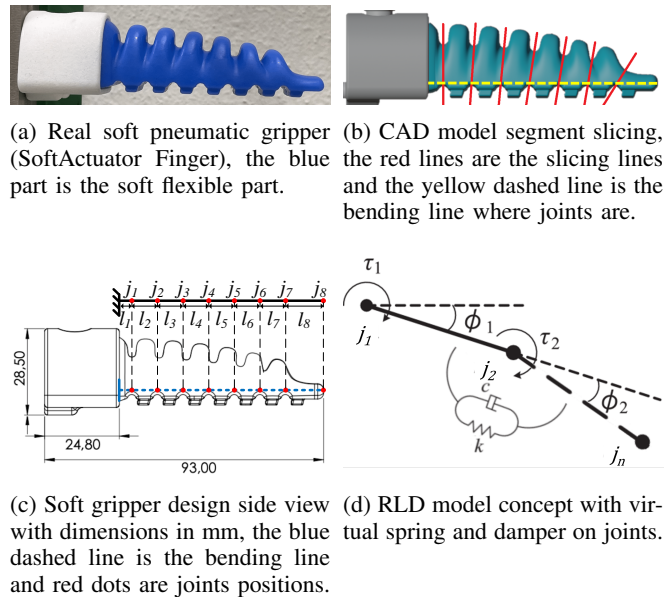
Our work offers a solution for harnessing the capabilities of the Webots robotic simulator in the study of beam-like soft robots that can be integrated or interact with rigid robots. This approach enables fully controllable and computationally efficient simulations of soft robots, coupled with an automatic calibration process to create comprehensive models integrated within an established robotic simulator.

II. MODELING APPROACH

To create lightweight simulation models with controllability features similar to those in robotic simulators for rigid-link robots, we develop our model directly within Webots. Webots is an open-source physics-based robotics simulator utilizing the Open Dynamics Engine (ODE) for simulating rigid body dynamics. Although Webots does not inherently support soft body dynamics, it includes a simulation environment parameter (CFM) that adjusts collision hardness, allowing rigid objects to pass through each other on impact. This provides a basic means to simulate the softness of contact points between solid objects.

In this study, our reference is an off-the-shelf beam-like pneumatically actuated soft gripper (SoftGripping SoftActuator Finger [11]) measuring roughly $68\text{mm} \times 20\text{mm} \times 22\text{mm}$ and weighing 20g, made from silicone rubber material as seen in Figure 2a. We simulate a beam-like soft robot using an RLD model, similar to previous works on [22], where segments are connected via hinge joints in Webots. First, we slice the soft gripper’s CAD model into several segments and consider the joints placed at the slicing locations as in Figure 2b. We assume the soft gripper bends primarily at the valley points. Since our soft gripper has seven gaps, thus eight rigid segments are created in the simulation model.

Webots has various types of virtual joints to simulate the connection between segments, such as single-axis hinge joints, dual-axis hinge joints, slider joints, and ball joints. In our simulation, each segment is connected with a hinge joint, allowing rotation around the axis perpendicular to the side plane of the segments. The hinge joint node in Webots allows



(a) Real soft pneumatic gripper (SoftActuator Finger), the blue part is the soft flexible part. (b) CAD model segment slicing, the red lines are the slicing lines and the yellow dashed line is the bending line where joints are.

(c) Soft gripper design side view with dimensions in mm, the blue dashed line is the bending line and red dots are joints positions. (d) RLD model concept with virtual spring and damper on joints.

Fig. 2: A depiction of (a) the real soft gripper, (b,c) CAD model slicing [11], and (d) the RLD model concept.

rotation along a main axis and is defined by two parameters: (i) the joint stiffness or spring constant (N.m/rad), and (ii) the joint friction or damping constant (N.m.s/rad). The spring constant controls the joint’s springiness, emulating a torsional spring. A higher spring constant means a stiffer joint that resists bending. The damping constant controls energy dissipation in the joint, applying a force proportional to the joint’s velocity: $F = -Bv$, where B is the damping constant and $v = \frac{dx}{dt}$ is the joint velocity calculated by the physics simulator. The hinge joint node also includes a rotational motor that can be actuated via torque input to control the joint angle. When it is actuated, the joint angle follows the motor input (active joint); otherwise (when not actuated), it responds to the net torque (passive joint) [23].

The mass-spring-damper system in Webots simulates a beam-like soft robot by linking rigid segments via hinge joints as shown in Figure 2d. These joints enable rotation around an axis and are characterized by joint stiffness (spring constant) and joint friction (damping constant) within Webots. We used the default softCFM value of 0.001. We add extra weight to the tip of the soft gripper to create a bending curve to measure the spring constant. We also bend the soft gripper to the initial position before suddenly releasing the soft gripper to measure the damping constant. For a given damping constant, the soft gripper’s static behavior is influenced by the spring constant; a higher spring constant makes the beam stiffer and less droopy. For a given spring constant, the soft gripper’s dynamic behavior is affected by the damping constant; a higher damping constant causes the beam to reach a steady state after a perturbation slowly with fewer oscillations. For the active behavior while the gripper is under pneumatic actuation, simulated by the rotational motor with torque constant in each joint within Webots. The torque constant determines the torque that applies in each

joint regarding the real pressure that is applied on the gripper. Section III details how we calibrate these parameters by comparing the static and dynamic behaviors of the simulated beam against those of a real soft beam.

III. CALIBRATION APPROACH

The calibration process involves finding model parameters to match measurements between real-world experiments and simulated ones. We consider passive (no pneumatic actuation) experiments for calibrating the spring and damping parameters and active (with pneumatic actuation) experiments for calibrating the torque parameters. We use simulations in Webots to compare and iteratively adjust the model parameters to align real and simulated behavior. This process involves using a Particle Swarm Optimization (PSO) method for optimization of the parameters and simulations in Webots, where each of the particles in the PSO swarm corresponds to a Webots simulation world.

A. Automatic Calibration Procedure

The primary objective of our calibration routine is to identify parameters that allow for the closest match of measurements between real-world experiments and simulated experiments in Webots. We use a PSO heuristic search algorithm to efficiently cover the search space for each experiment. PSO is inspired by the social behavior of birds and fish, and finds locally optimal solutions through collaboration among particles in a multidimensional search space [24]. In this approach, each individual within the population, referred to as a particle, represents a distinct instance of our simulated world characterized by a specific set of parameters for the RLD model. Each particle's position x_i and velocity are initialized randomly on an appropriate range. Thereafter, in each iteration, the fitness of each particle is assessed through a measure that is able to capture the similarity between real-world experiments and simulated ones. Subsequently, in each iteration, each particle's position and velocity are updated:

$$\mathbf{v}_i(t+1) = \omega \mathbf{v}_i(t) + c_1 r_1 (\mathbf{p}_i - \mathbf{x}_i(t)) + c_2 r_2 (\mathbf{g} - \mathbf{x}_i(t)) \quad (1)$$

$$\mathbf{x}_i(t+1) = \mathbf{x}_i(t) + \mathbf{v}_i(t+1) \quad (2)$$

where ω is the inertia weight, c_1 and c_2 are cognitive and social coefficients, r_1 and r_2 are random numbers uniformly distributed in $[0, 1]$, \mathbf{p}_i is a particle's personal best and \mathbf{g} is the global best position. We use an implementation of PSO found in the pyswarms library [25], outlined in Algorithm 1.

The calibration routine is automated using Python scripts. The parameters for the calibration are loaded from a JSON file (parameters.txt). This file contains critical information such as the type of calibration (spring or damping), and optimizer settings. To enhance the efficiency of the calibration process, multi-threading is employed. This allows multiple simulations to run concurrently, leveraging the computational power of modern multi-core processors. Threads are controlled with a locking mechanism to ensure that fitness calculations are synchronized and that each particle's fitness score is accurately updated.

Algorithm 1 Particle Swarm Optimization (PSO)

Initialization:

for each particle i **do**

 Initialize position vector \mathbf{x}_i and velocity vector \mathbf{v}_i

 Set best-known position \mathbf{p}_i to initial position \mathbf{x}_i

end for

PSO iterations:

while termination criterion not met **do**

for each particle i **do**

 Update velocity

 Update position

end for

for each particle i **do**

 Evaluate fitness using the objective function

end for

end while

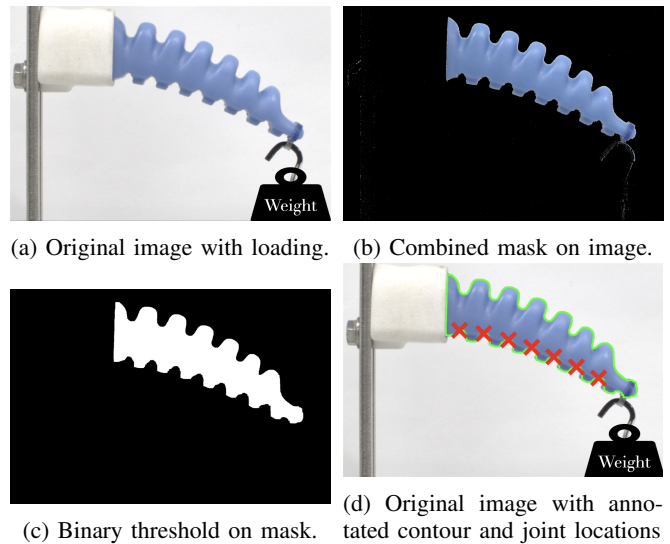


Fig. 3: Image processing steps to assign the joint locations.

B. Passive Calibration Experiments

Passive calibration determines model parameters by subjecting the gripper to an external load without pneumatic actuation to analyze its static and dynamic response. We conduct static and dynamic passive experiments with the gripper positioned downward as seen in Figure 3.

In a first step, we calibrate the spring constant of the soft gripper in a static experiment by subjecting the gripper to an external load at the tip. An image is then taken using a camera setup at a fixed distance and angle with respect to the soft gripper. The images are processed to obtain the rotational angle of each joint. This experiment is repeated with various weights added to the tip of the gripper. A virtual position sensor is used to measure a joint's angle within Webots.

The image processing workflow begins by converting the original image to grayscale and applying a threshold to isolate non-white elements. The original image is then transformed into the HSV color space, and a mask is applied to retain only the gripper's hue, saturation, and value within a

specified range. Advantages of using HSV are that it presents immunity to illumination changes and the color hue changes are continuous and linear [26]. This HSV mask is combined with the grayscale threshold mask and applied to the original image. The resulting image is further processed by converting it to a binary grayscale format to clearly outline the gripper's shape. Additional morphological operations like dilation and erosion can be performed to reduce noise and better define object boundaries [27] [28]. In the binary image, the contour of the gripper, defined as the curve that joins all continuous points with the same color or intensity, is detected using OpenCV's `findContours` function [29]. The contour is split to obtain the bottom- and top line of the contour by selecting the minimal and maximal x-value. Finally, the peaks of the bottom contour, representing joint locations, are identified through comparison of neighboring values [30], and the angles between these joints are calculated following:

$$\theta_i = \begin{cases} \arctan\left(\frac{-\Delta y_i}{\Delta x_i}\right) & \text{if } i = 1 \\ \arctan\left(\frac{-\Delta y_i}{\Delta x_i}\right) - \sum_{j=1}^{i-1} \theta_j & \text{if } i > 1 \end{cases} \quad (3)$$

where (x, y) represents the location of a joint and $\theta_i \in [-\frac{\pi}{2}, \frac{\pi}{2}]$ is the i^{th} joint angle. These steps are shown in Figure 3.

The fitness of a parameter set is computed as the mean squared error of the difference in joints' simulated and real angular position:

$$\text{Fitness} = \frac{1}{N} \sum_{j=1}^N (\phi_j^{\text{sim}} - \phi_j^{\text{real}})^2 \quad (4)$$

where N is the number of joints, ϕ_j^{sim} is the angle of joint j in the simulation, and ϕ_j^{real} is the angle of joint j in the real experiment. Lower values denote a closer matching.

In the second step, we calibrate the damping constant of the soft gripper's joints in the dynamic experiment. The gripper is subjected to a step load and we compare the gripper's settling time and number of overshoots. In the real experiment, we apply a load on the gripper's tip as an initial condition and then instantly remove the load to observe the settling behavior of the gripper. In the simulated experiment, we replicate similar conditions using a virtual load applied at the tip. Webots does not allow for the releasing of an object, instead, we first obtain the joint angles in an initial simulation and use these as an initial condition in subsequent experiments to observe the settling behavior of the gripper.

The gripper's response is measured by tracking the vertical position of the corner with the highest x-value in a video recording. To capture the grippers behavior, the Sony ZV-1 camera was used [31]. An effective frame rate of 960-1000 frames per second was employed. In real experiments, this is done using an automated video processing function that detects the gripper's contour in each frame with the aforementioned techniques. In simulated experiments, the location is obtained by using a forward kinematics scheme from the rotational angles in the joints and the length between them. The detected y-positions of the real experiment are smoothed with a Gaussian filter [32], and key extrema

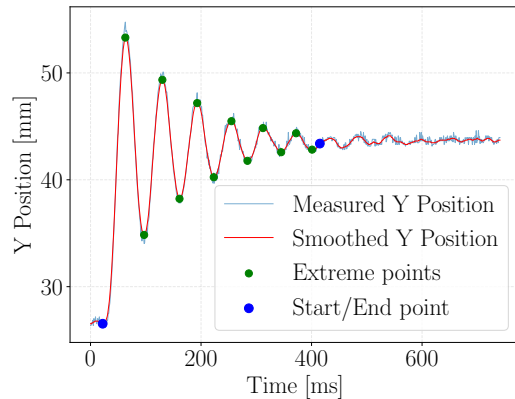


Fig. 4: Settling behavior of the gripper after instantaneous release of an added weight at the tip: Before release, the gripper was subjected to 40 grams of added weight to the tip. The number of overshoots in this experiment was 12 and the settling time 0.409 seconds.

(peaks and valleys) are identified to count overshoots and measure settling time [30]. We count an overshoot if the vertical distance between two overshoots is more than 1 millimeter. An example of the overshoot counting is plotted in Figure 4.

The fitness between the real-world and simulated experiments is computed as the following:

$$\text{Fitness} = |T_s^{\text{sim}} - T_s^{\text{real}}| (1 + |n_o^{\text{sim}} - n_o^{\text{real}}|) \quad (5)$$

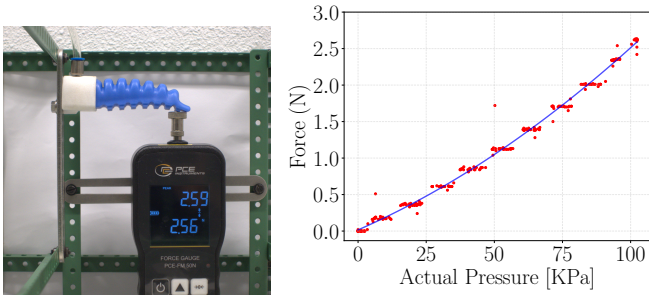
where T_s^{sim} and T_s^{real} represent the simulated and real settling times and n_o^{sim} and n_o^{real} represent the number of overshoots in simulation and reality, respectively.

C. Active Calibration Experiments

In active calibration experiments, we study the behavior of the gripper under pneumatic actuation to find torque parameters. The gripper is operated through pressurized air, where increasing pressure leads to flexing, and decreasing it results in the extension of the gripper. Active calibration involves applying forces and gauging the response to validate the soft gripper's torque parameters. We applied pressurized air as an input for the real experiment between 0-100 KPa. We use virtual rotational motor torque to actuate the gripper in the simulator. The experimental setup is shown in Figure 5. The input variables for calibration encompass applied force, spring constant, and damping. Output variables determining the fitness function for optimization involve force at the tip and deformation. We used a scale to measure the force on the tip in the real experiment and a virtual force sensor in the simulation. As shown in Figure 5, the relationship between the applied pressure and the force exerted at the tip is approximately linear, consistent with previous research [22]. Thus, we model the joint torque as:

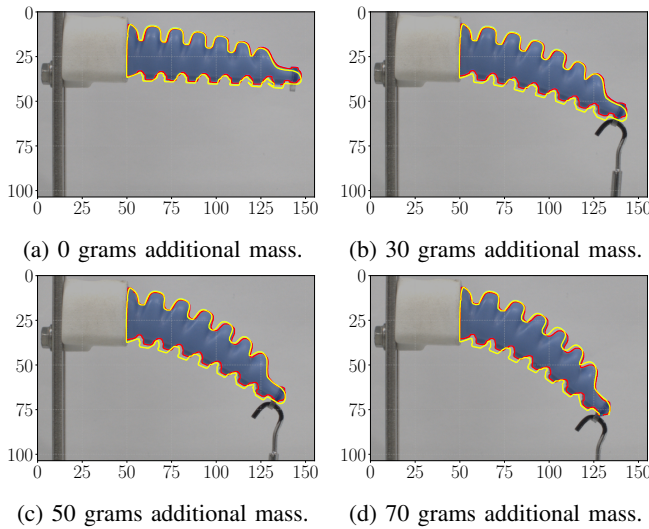
$$\tau_i = \alpha_i P \quad (6)$$

where τ_i [Nm] is the torque applied at joint i , α_i [$\frac{1}{m^2}$] is the parameter to be calibrated, and P [Pa] is the applied pressure.



(a) Force measurement at the gripper's tip with 100 KPa input air pressure. (b) Relationship between the applied pressure and the exerted force at the tip of the gripper

Fig. 5: Active experiment force measurements.



(a) 0 grams additional mass. (b) 30 grams additional mass. (c) 50 grams additional mass. (d) 70 grams additional mass.

Fig. 6: Validation of calibration routine for passive static experiments: Soft gripper subjected to a load in the real-world experiment with a contour overlay of its simulated counterpart with identical load. The red line indicates the contour obtained from the real-world image, while the yellow line represents the contour derived from the Webots simulation analysis. Both axes are measured in millimeters.

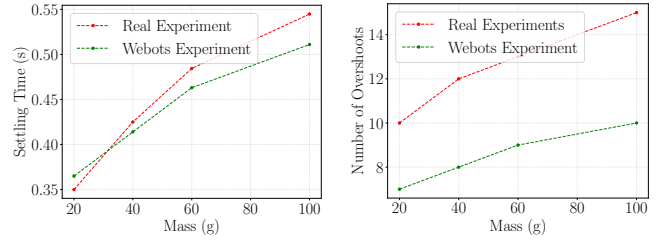
The fitness score is calculated as the difference between the force applied at the tip in real and simulation experiments:

$$\text{Fitness} = |F^{\text{sim}} - F^{\text{real}}| \quad (7)$$

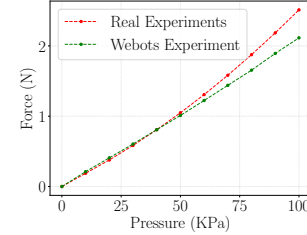
where F^{sim} and F^{real} are the force that is exerted by the virtual gripper and real gripper respectively.

IV. EXPERIMENTAL SETUP AND RESULTS

Passive experiments were carried out with the gripper positioned in the downward direction. Figure 3a illustrates the gripper undergoing stimulation with additional weights. First, we calibrate the spring constant of the soft gripper using unstimulated and stimulated using various added weights from 10 to 100 grams. We capture an image for each different weight. The optimization process is shown in Figure 8a and



(a) Settling time comparison. (b) Overshoots comparison.



(c) Force-pressure comparison.

Fig. 7: Validation of calibration routines for passive dynamic (a,b) and active experiments (c). For the passive dynamic experiment validation, settling times and the number of overshoots were analyzed under different externally applied loads. In the active experiment validation, the exerted force at the gripper's tip was compared across various applied pressures and corresponding torque coefficients in Webots.

Figure 9a. During the automatic calibration routine, we use added weights of 0, 20, and 40 grams, and the results are validated with 30, 50, and 50 grams of added weight. The validation showed a similarity between the real and simulated gripper as illustrated in Figure 6.

Second, we calibrate the damping constant of the soft gripper by subjecting it to an initial load condition of 20 and 40 grams and instantly release the weight to an unweighted condition. We record a video for each different added weight condition. The optimization process is shown in Figure 8b and Figure 9b. We achieve a converged fitness function 5 and parameters for damping. The results are validated in terms of the difference in settling time and number of overshoots, in Figure 7b and Figure 7a. It can be noted that the difference in settling time is small. While the trend is the same, there is still some difference in the number of overshoots.

Next, We calibrate the torque constant in each joint of the soft gripper by comparing the force measured on the tip through the active calibration. We actuated the gripper with various air pressures from 0 to 100 KPa with 10 KPa resolution. We measured the force at the tip for 20 iterations for each pressure condition through force gauge (PCE-FM 50N) readings as shown in Figure 5a. The optimization process is shown in Figure 8c and Figure 9c. We use the previously acquired spring and damping parameters to conduct the active experiments simulation in Webots. We validated the results by applying a range of pressures and measuring the difference in exerted force in the real- and Webots experiments. The validation results are shown in

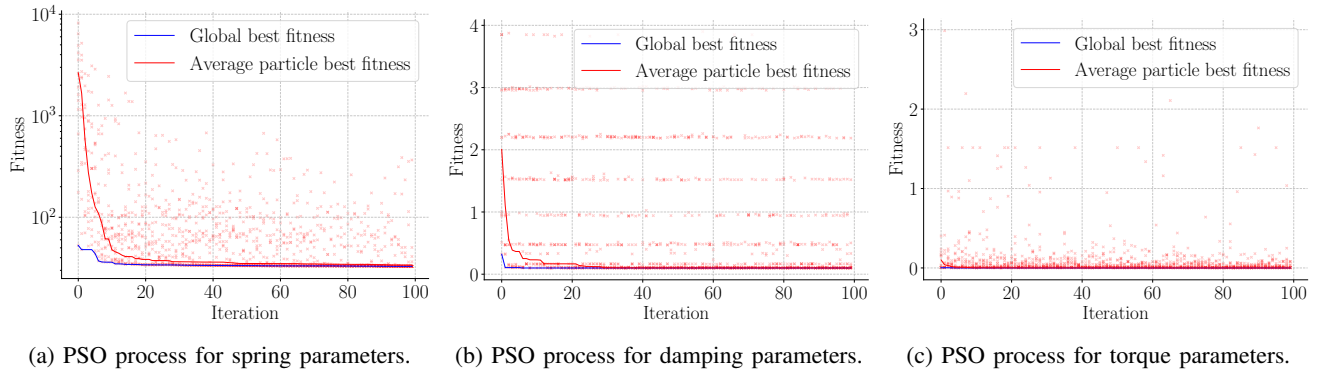


Fig. 8: We perform calibration using a PSO method to obtain model parameters of spring, damping, and torque. The line and scatter plot show the fitness evolution of particles during the PSO process.

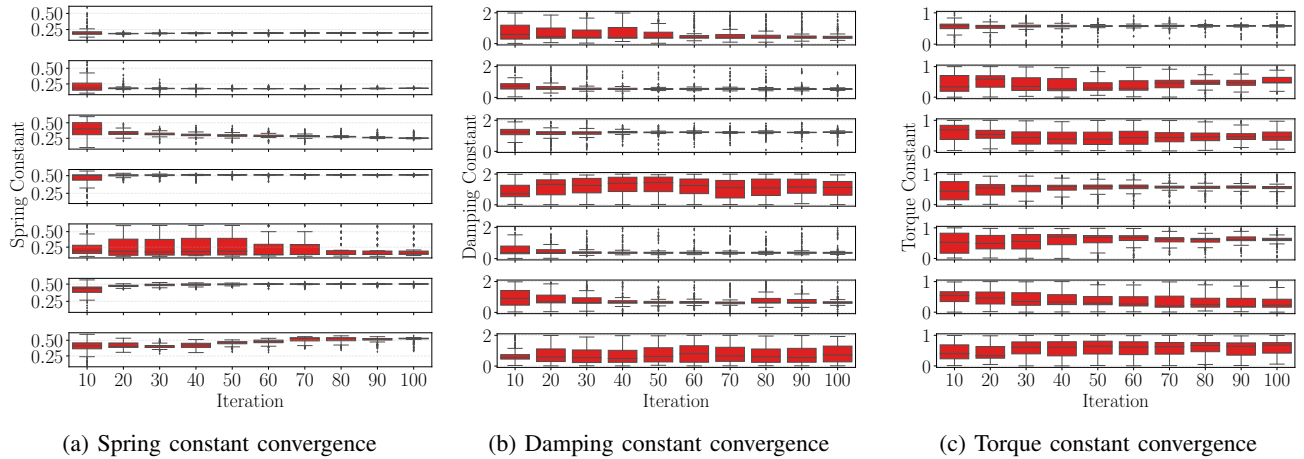


Fig. 9: Box plots illustrating the distribution of calibrated parameters over iterations for each joint during the PSO process. The personal best solutions of all particles are grouped and averaged every 10 iterations.

Figure 7c. We use 100 PSO iterations for all parameters. All the final acquired parameters of spring, damping, and torques after the PSO optimization are shown in Table I.

V. CONCLUSION AND OUTLOOK

In this work, we presented a method for simulating pneumatically actuated, beam-like soft robotic grippers within the Webots simulation environment using an RLD model. Leveraging a PSO method, we identified optimal parameters for spring, damping, and torque to replicate the physical behaviors of the real gripper with high fidelity, achieving close alignment with real-world experiments. This approach

TABLE I: The optimal model parameters found through PSO, the spring (k), damping (c), and torque (α) constants.

Parameters \ Joints	Joints						
	1	2	3	4	5	6	7
k [$\frac{\text{Nm}}{\text{rad}}$]	0.190	0.176	0.311	0.517	0.103	0.484	0.401
c [$10^{-3} \cdot \frac{\text{Nms}}{\text{rad}}$]	0.511	0.405	1.217	0.791	0.227	0.248	0.281
α [$10^{-6} \cdot \frac{1}{\text{m}^2}$]	0.279	0.375	0.372	0.507	0.486	0.421	0.482

effectively expands Webots' utility, facilitating studies where soft robots are integrated with rigid-body systems.

Moving forward, we aim to enhance the model's versatility by developing an automated segmentation program to generalize this approach for various soft robotic designs, enabling a wider range of applications of our approach to various grippers. Additionally, refining PSO fitness functions could yield even greater simulation accuracy across diverse morphologies and actuation types, improving precision in the model's physical representations. These advancements will further support increasingly complex studies on soft robotic grippers integrated with rigid robots (typically an arm), reducing dependency on specialized simulation environments and broadening potential research applications.

In summary, our framework offers a streamlined, versatile approach to simulating soft robotic grippers. This work paves the way for expanded adoption of hybrid robotic simulations and next-generation soft robotic systems that can seamlessly interact with rigid elements in both virtual and practical settings. All of our software is made available open-source.

ACKNOWLEDGMENT

This work was partially supported by the Indonesian Education Scholarship from the Center for Financing of Higher Education (BPPT) and the Indonesia Endowment Fund for Education (LPDP).

REFERENCES

- [1] B. Mazzolai, L. Margheri, M. Cianchetti, P. Dario, and C. Laschi, "Soft-robotic arm inspired by the octopus: II. from artificial requirements to innovative technological solutions," *Bioinspiration and biomimetics*, vol. 7, no. 2, p. 025005, 2012.
- [2] D. Rus and M. T. Tolley, "Design, fabrication and control of soft robots," *Nature*, vol. 521, no. 21, pp. 467–475, 2015. [Online]. Available: <https://doi.org/10.1038/nature14543>
- [3] V. Falkenhahn, T. Mahl, A. Hildebrandt, R. Neumann, and O. Sawodny, "Dynamic modeling of constant curvature continuum robots using the Euler-Lagrange formalism," in *2014 IEEE/RSJ International Conference on Intelligent Robots and Systems*, Sep. 2014, pp. 2428–2433, iSSN: 2153-0866. [Online]. Available: <https://ieeexplore.ieee.org/document/6942892>
- [4] K. C. Galloway, K. P. Becker, B. Phillips, J. Kirby, S. Licht, D. Tchernov, R. J. Wood, and D. F. Gruber, "Soft Robotic Grippers for Biological Sampling on Deep Reefs," *Soft Robotics*, vol. 3, no. 1, pp. 23–33, 2016. [Online]. Available: <https://www.liebertpub.com/doi/10.1089/soro.2015.0019>
- [5] J. F. Elfferich, D. Dodou, and C. D. Santina, "Soft Robotic Grippers for Crop Handling or Harvesting: A Review," *IEEE Access*, vol. 10, pp. 75 428–75 443, 2022. [Online]. Available: <https://ieeexplore.ieee.org/document/9829727/>
- [6] S. Abondance, C. B. Teeple, and R. J. Wood, "A Dexterous Soft Robotic Hand for Delicate In-Hand Manipulation," *IEEE Robot. Autom. Lett.*, vol. 5, no. 4, pp. 5502–5509, Oct. 2020. [Online]. Available: <https://ieeexplore.ieee.org/document/9134855/>
- [7] C. Laschi, M. Cianchetti, B. Mazzolaia, L. Margheri, M. Follador, and P. Dario, "Soft robot arm inspired by the octopus," *Advanced Robotics*, vol. 26, no. 7, pp. 709–727, 2012. [Online]. Available: <https://doi.org/10.1163/156855312X626343>
- [8] R. K. Katzschmann, A. D. Marchese, and D. Rus, "Hydraulic autonomous soft robotic fish for 3d swimming," in *Experimental Robotics*. Springer International Publishing, 2016, vol. 109, pp. 405–420, series Title: Springer Tracts in Advanced Robotics. [Online]. Available: http://link.springer.com/10.1007/978-3-319-23778-7_27
- [9] N. Koenig and A. Howard, "Design and use paradigms for gazebo, an open-source multi-robot simulator," in *2004 IEEE/RSJ International Conference on Intelligent Robots and Systems (IROS) (IEEE Cat. No.04CH37566)*, vol. 3, 2004, pp. 2149–2154 vol.3.
- [10] O. Michel, "Cyberbotics Ltd. webots™: Professional mobile robot simulation," *International Journal of Advanced Robotic Systems*, vol. 1, no. 1, p. 5, 2004. [Online]. Available: <https://doi.org/10.5772/5618>
- [11] *Operating Instruction SoftGripper and SoftActuators*, SoftGripping, 2023, rev. 2.1.
- [12] P. Moseley, J. M. Florez, H. A. Sonar, G. Agarwal, W. A. Curtin, and J. K. Paik, "Modeling, design, and development of soft pneumatic actuators with finite element method," *Advanced Engineering Materials*, vol. 18, 2016. [Online]. Available: <https://onlinelibrary.wiley.com/doi/abs/10.1002/adem.201500503>
- [13] Y. Hu, J. Liu, A. Spielberg, J. B. Tenenbaum, W. T. Freeman, J. Wu, D. Rus, and W. Matusik, "Chainqueen: A real-time differentiable physical simulator for soft robotics," in *2019 International Conference on Robotics and Automation (ICRA)*, 2019, pp. 6265–6271.
- [14] C. Armanini, I. Hussain, M. Z. Iqbal, D. Gan, D. Prattichizzo, and F. Renda, "Discrete cosserat approach for closed-chain soft robots: Application to the fin-ray finger," *IEEE Transactions on Robotics*, vol. 37, no. 6, pp. 2083–2098, 2021.
- [15] B. J. Caasenbrood, A. Y. Pogromsky, and H. Nijmeijer, "Energy-shaping controllers for soft robot manipulators through port-hamiltonian cosserat models," *SN Computer Science*, vol. 3, pp. 1–12, 2022. [Online]. Available: <https://link.springer.com/article/10.1007/s42979-022-01373-w>
- [16] C. Rad, O. Hancu, and C. Lapusan, "Data-driven kinematic model of pneunets bending actuators for soft grasping tasks," *Actuators*, vol. 11, no. 2, 2022. [Online]. Available: <https://www.mdpi.com/2076-0825/11/2/58>
- [17] P. Ferrentino, E. Roels, J. Brancart, S. Terryn, G. Van Assche, and B. Vanderborght, "Finite element analysis-based soft robotic modeling: Simulating a soft actuator in sofa," *IEEE Robotics & Automation Magazine*, pp. 2–12, 2023.
- [18] M. A. Graule, C. B. Teeple, T. P. McCarthy, G. R. Kim, R. C. St. Louis, and R. J. Wood, "Somo: Fast and accurate simulations of continuum robots in complex environments," in *2021 IEEE/RSJ International Conference on Intelligent Robots and Systems (IROS)*, 2021, pp. 3934–3941.
- [19] M. Bednarek, P. Kicki, J. Bednarek, and K. Walas, "Gaining a sense of touch object stiffness estimation using a soft gripper and neural networks," *Electronics*, vol. 10, no. 1, 2021. [Online]. Available: <https://www.mdpi.com/2079-9292/10/1/96>
- [20] B. J. Caasenbrood, A. Y. Pogromsky, and H. Nijmeijer, "Sorotoki: A matlab toolkit for design, modeling, and control of soft robots," *IEEE Access*, vol. 12, pp. 17 604–17 638, 2024.
- [21] A. T. Mathew, I. B. Hmida, C. Armanini, F. Boyer, and F. Renda, "Sorosim: A matlab toolbox for hybrid rigid–soft robots based on the geometric variable-strain approach," *IEEE Robotics & Automation Magazine*, vol. 30, no. 3, pp. 106–122, 2023.
- [22] Z. Wang and S. Hirai, "Soft gripper dynamics using a line-segment model with an optimization-based parameter identification method," *IEEE Robotics and Automation Letters*, vol. 2, no. 2, pp. 624–631, 2017.
- [23] Cyberbotics Ltd., *RotationalMotor — Webots Documentation*, 2024. [Online]. Available: <https://cyberbotics.com/doc/reference/rotationalmotor>
- [24] R. Poli, J. Kennedy, and T. Blackwell, "Particle swarm optimization: An overview," *Swarm intelligence*, vol. 1, pp. 33–57, 2007.
- [25] L. J. Miranda, "Pyswarms: a research toolkit for particle swarm optimization in python," *Journal of Open Source Software*, vol. 3, no. 21, p. 433, 2018. [Online]. Available: <https://doi.org/10.21105/joss.00433>
- [26] E. Chavolla, D. Zaldivar, E. Cuevas, and M. A. Perez, "Color spaces advantages and disadvantages in image color clustering segmentation," *Advances in soft computing and machine learning in image processing*, pp. 3–22, 2018.
- [27] K. A. M. Said, A. B. Jambek, and N. Sulaiman, "A study of image processing using morphological opening and closing processes," *International Journal of Control Theory and Applications*, vol. 9, no. 31, pp. 15–21, 2016.
- [28] P. T. Jackway and M. Deriche, "Scale-space properties of the multiscale morphological dilation-erosion," *IEEE transactions on pattern analysis and machine intelligence*, vol. 18, no. 1, pp. 38–51, 1996.
- [29] OpenCV Documentation, "Contours - opencv python tutorials," https://docs.opencv.org/4.x/d4/d73/tutorial_py_contours_begin.html, 2024.
- [30] SciPy Documentation, "scipy.signal.find_peaks — scipy v1.11.2 manual," <https://docs.scipy.org/>, 2024.
- [31] "Sony zv-1 compact camera," <https://www.sony.nl/compact-cameras/products/zv-1>.
- [32] SciPy Documentation, "scipy.ndimage.gaussian.filter," <https://docs.scipy.org/>, 2024.